Vision Res. Vol. 32, No. 4, pp. 645–656, 1992
Printed in Great Britain. All rights reserved

0042-6989/92 $5.00 + 0.00
Copyright © 1992 Pergamon Press plc

Scotopic Visual Efficiency: Constraints by Optics, Receptor Properties, and Rod Pooling*

GARY L. SAVAGE,†‡ MARTIN S. BANKS†

Received 16 January 1991; in revised form 26 August 1991

We studied the influence of optics, photoreceptor properties, and rod pooling on scotopic contrast sensitivity by comparing the performance of an ideal discriminator to that of human observers. Comparisons of human and ideal contrast sensitivities indicated that preretinal factors and summation area were not sufficient to explain the shape of the human CSF. Spatial pooling of rods was explored as a possible explanation of this discrepancy. Our highest efficiency, expressed in terms of a human/ideal contrast sensitivity ratio, was about 1:3 (0.33) for a contrast discrimination task.

Scotopic Efficiency Rods Detection Contrast sensitivity Summation area Ideal observer Quantum efficiency

INTRODUCTION

In 1942 Hecht, Shlaer and Pirenne found that the minimum detectable quantity of light produced only 5–14 photon absorptions by the rods. Their stimulus covered about 500 rods by their estimate, so the probability that one rod absorbed 2 or more photons was considered very small. In other words, Hecht and colleagues showed that at absolute threshold a rod can be activated by the absorption of a single photon. Their computations showed that a total of 5–8 "simultaneous" retinal events appeared to be utilized by their subjects, a range very close to their photometric estimate of 5–14 isomerizations per flash. The close correspondence between the photometric and psychophysical estimates led them to conclude that biological variability (under their conditions) was very low. Their remarkable report has served as a benchmark for subsequent analyses of the efficiency of human vision (Rose, 1948; Bouman, 1955; Barlow, 1956, 1957, 1958, 1962a,b, 1977; Jones, 1959; Sakitt, 1972; van Meeteren & Boogaard, 1973; van Meeteren, 1978; Hallett, 1969, 1987).

Although the number of photon absorptions required at absolute threshold is quite small, it does not necessarily follow that these are conditions under which photons are used most efficiently. Barlow (1962b) questioned whether briefly flashed, sharply focused spots of light were necessarily well-matched to the temporal and spatial weighting functions used by the retina. Could more efficient conditions exist?

The answer to this question has major implications for our understanding of how the visual system works. Rose (1948) emphasized that the gap between human and ideal behavior is a measure of the "logical space" within which one can postulate mechanisms other than quantum fluctuations as limitations of performance. Likewise, Barlow (1962b) pointed out that the greatest information on visual mechanisms is obtained where efficiency is the highest; i.e. there are a multitude of plausible inefficient mechanisms, but comparatively few efficient ones.

Watson, Barlow and Robson (1983) and Crowell and Banks (1992) investigated the conditions under which foveally-presented, photopic gratings are detected most efficiently. Watson *et al.* calculated efficiency by comparing human performance to that of an ideal observer placed at the cornea. They found that efficiency was best for 6–8 cycles per degree (cpd) grating patches. Under those conditions, quantum efficiency was about 0.0005, which corresponds to a ratio of human/ideal contrast sensitivity of just over 0.02. With an ideal observer placed at the outputs of the photoreceptors, Crowell and Banks (1992) found that the ratio of human/ideal sensitivity increased to 0.1–0.2 for grating patches of 5–48 cpd. The fact that this ratio was constant over this range of spatial frequencies suggested that the high-frequency slope of the foveal contrast sensitivity function (CSF) under photopic viewing conditions can be explained by an analysis of information loss caused by the eye's optics, photoreceptor properties, and grating summation effects (see also Banks, Geisler & Bennett, 1987; Howell & Hess, 1978). In the present study, a similar analysis for scotopic vision will be developed.

*Part of this paper served as the first author's Ph.D. dissertation and was presented at 1988 Meeting of the Association for Research in Vision and Ophthalmology.

†University of California at Berkeley, School of Optometry, Berkeley, CA 94720, U.S.A.

‡To whom all correspondence should be addressed at present address: University of Houston, College of Optometry, Houston, TX 77204, U.S.A.

Efficiency generally seems to worsen with increasing light level (Barlow, 1962b), so visual performance probably approaches the limits imposed by photon noise (i.e. ideal performance) most closely at scotopic luminances. In the interest of quantifying how efficiency at low light levels varies with luminance and spatial frequency, human performance was compared to that of an ideal observer under scotopic conditions.

The ideal observer was constructed in the fashion of Geisler (1984, 1989) with the optics and rods of human observers. We find that scotopic efficiency declines significantly as retinal illuminance is raised from -2.5 to -0.2 log scot td, the range of illuminances tested. As will be discussed later, human sensitivity might, in fact, be expected to approach ideal most closely at some mid-scotopic illuminance level rather than at absolute threshold.

Scotopic efficiency also declines with increasing spatial frequency; efficiency plummets above 0.3 cpd at -2.5 log scot td and above 1 cpd at -0.2 scot td. This means that the high-frequency slope of the human scotopic CSF cannot be explained by information loss in optics and rod receptors alone at any of the light levels tested. Finally, scotopic efficiency is significantly higher than photopic efficiency over a broad range of light levels and spatial frequencies.

GENERAL METHODS

Stimuli

The stimuli for all experiments were generated with a Raster Technologies One/80 graphics processor, hosted by a PDP 11/73. They were presented on a Conrac 7311 color monitor with a spatial resolution of 1280×1024 and a frame rate of 60 Hz (non-interlaced). The monitor was run in a grayscale mode by applying voltages computed for the green gun to the blue and red guns also. The unfiltered "equal gun value white" at a photopic luminance of 59 cd/m^2 resembled P4 phosphor at a similar luminance. A dark surround mask, placed on the monitor to block stray light, yielded a visible raster of 36×27 cm. Viewing distance varied from 0.31 to 2.5 m depending on the desired spatial frequency.

The stimuli for the grating summation experiment were square patches of horizontal sinewave gratings in sine phase. They had a width and height of 1, 2, 4, 6, 8 or 12 cycles. These gratings were truncated at zero crossings along the horizontal edges and were Gaussian-damped (SD = 0.5 cycles) on the ends of the bars. The largest square grating came within about 2 cm of the upper and lower edges of the screen mask and within 7 cm of its lateral edges.

The stimuli for the CSF experiment were horizontally-oriented Gabor patches in sine phase. Their luminance distributions are described by the standard equation:

$$f(x,y) = \mathrm{m} \cdot \sin(b \cdot y) \cdot \exp\{-[(x/s)^2 + (y/s)^2]\} + L_0.$$

Note that the standard deviations for the vertical and horizontal Gaussians were always equal; i.e. the aspect ratio was 1.0.

The temporal waveform was a rectangular pulse of 100 msec duration in all of the present experiments. A brief experiment showed that human performance most closely approached ideal for durations of 100–150 msec over the range of spatial frequencies utilized.

Calibration

Stimulus measurements were conducted with a Pritchard Spectrophotometer equipped with scotopic and photopic filters as well as an SC-80A Micro-Scanner. A linear contrast response was produced by "linearizing" software based on individual luminance calibrations of each color gun. Correspondence of input to output contrast was excellent ($\pm 5\%$ of desired values) from 5 to 90% contrast for spatial periods of 20 pixels or more.

Subjects and apparatus

The two observers had normal vision and were both about 40 yr old. One observer, the first author, was experienced in psychophysical experiments and the other was not. Both were tested monocularly with optimum foveal refractive correction (for the given test distance). The pupil was dilated and accommodation paralyzed with 0.5% cyclopentolate. Pupil diameters were 8.5 and 7.5 mm for observers GS and SS, respectively. Before each session, the observer was dark-adapted for 50 min and allowed to adapt to the background light level for at least 3 min.

We wished to test near the density peak of the rod distribution and to avoid retinal areas containing macular pigment. Consequently, stimuli were presented at 20 deg in the nasal visual field. A red LED served as the fixation target. It was rendered barely visible by filters placed before the observer's eye.

A bite bar stabilized the observer's head to help maintain alignment with a trial lens/filter holder. A cloth and cardboard hood was used to eliminate stray light. Viewing distance and fixation target position were varied to achieve the desired spatial frequency and target eccentricity.

Control of light level

Space-average luminance was varied by placing Wratten neutral density (ND) filters before the observer's eye and/or by putting ND filter material in front of the monitor. A Wratten 47B (blue) filter was also placed before the eye. All ND filters were calibrated in combination with the Wratten 47B. With this filter combination, a 3 log-unit range of scotopic luminances was produced.

Psychophysical method

A two-interval forced-choice procedure with the method of constant stimuli was used to estimate contrast thresholds. Four different contrast levels separated by 0.1 log units were used in each condition, and the 0.3 log unit range was centered on the current best estimate of threshold. Percentages correct for each of the four log contrast values were subjected to probit analysis

to estimate the contrast associated with 75% correct. Twenty-five to fifty trials were presented at each contrast for a total of 100–200 trials per psychometric function. Standard errors were calculated from the probit output for each function. Two or three psychometric functions were measured for each condition. The thresholds estimated from each psychometric function were averaged to obtain the final estimate of threshold. Each data point, therefore, represents 200–600 observations.

Verification of rod isolation

We wished to test over as large a range of luminances as possible under conditions of rod isolation. Absolute threshold for peripheral cones and uniform test fields is about 0.3 (or −0.52 log) phot td (Daitch & Green, 1969). To test near this level of retinal illuminance while minimizing the possibility of cone intrusion, a Wratten 47B filter was substituted for about 1 log unit of ND material. This maneuver did not alter the scotopic retinal illuminance, but it reduced the photopic troland values more than a log unit below the reported cone threshold. This blue filter was used for all subsequent measurements.

To assure that cones did not contribute to detection under our conditions, two control experiments were conducted at our highest (putatively scotopic) light level of −0.21 log scot td. The first experiment tested the possibility that long-wavelength-sensitive (L) or medium-wavelength-sensitive (M) cones contributed and the other the possibility that short-wavelength-sensitive (S) cones did.

In the first control experiment, the −0.21 log scot td light level, or, −1.7 log phot td, was initially produced by viewing the screen through the combination of 3 log units of ND filters with the Wratten 47B (blue) filter. Contrast sensitivity was measured under this condition at 0.25 and 0.70 cpd with 4-cycle Gabor patches. Substituting 5.2 log units of ND for the combination of 3 ND with the 47B did not alter the photopic retinal illuminance; that is, both conditions yielded −1.7 log phot td. This substitution did reduce the scotopic retinal illuminance, however, by an additional 1.2 log units from −0.21 to about −1.4 log scot td. Contrast sensitivities were then re-measured for this condition. If only L and M cones determined sensitivity, the exchange should not have affected contrast sensitivity because the two conditions were photopically equated. On the other hand, if only rods determined sensitivity, there should have been a predictable decrease in sensitivity. Our testing over a 4 log unit range of low light levels (vide post) indicated that human contrast sensitivity decreased about 0.25 log unit for every log unit decrease in retinal illuminance. Thus, for the 1.2 log unit decrease in scotopic retinal illuminance produced by the filter substitution, one would have expected a decrease in sensitivity of about 0.3 log units. Our contrast sensitivities decreased by 0.3 log units, precisely the amount predicted if rods alone determined sensitivity. Two other observations are consistent with the claim that rods, and not L or M cones, mediated response at the highest light level. First, the screen appeared a "colorless" gray at this level. Retinal illuminance had to be increased by almost a log unit before the screen appeared bluish when viewed through the 47B filter. This suggested that cones did not intrude at the highest level tested. Second, measurement of absolute threshold indicated that our highest scotopic level was only about 2.5 log units above absolute threshold. A 2.5–3 log-unit range of pure scotopic vision would be expected for the relatively short wavelengths utilized here (Wald, 1945).

The second control experiment examined the possibility that S cones contributed to detection. We looked for evidence of S cone intrusion in two ways. First, the stimuli were equated for rod activation using two broadband filters (Wratten 47B and 65A) which produced quite different S cone stimulation. These stimuli yielded identical contrast thresholds. Second, stimuli equated for S cone activation, but not rod activation, were found to yield quite different contrast thresholds.

The results from the two control experiments demonstrated that L, M and S cones did not contribute to the thresholds measured in the experiments presented here.

The ideal discriminator

Various ideal observers have been employed in attempts to quantify the efficiency of real observers. For example, Watson *et al.* (1983) computed ideal performance for the detection of Gabor patches at photopic light levels. Their ideal observer was based on the energy distribution of the stimulus at the plane of the cornea. They compared human performance to those of this ideal observer. Another ideal observer was developed by Geisler (1984, 1989; Geisler & Davila, 1985). This ideal discriminator was specifically designed to allow the quantitative assessment of the influences of pre-neural factors on the detection and discrimination of a wide variety of spatial stimuli. The ideal discriminator has complete knowledge of every aspect of each stimulus. Photon noise is the only limit to the performance of the Stimuli Defined Exactly (SDE) observer. In order to discriminate stimulus pairs, the ideal discriminator applies an optimal weighting function to the distribution of photon absorptions across the receptor lattice.

We used Geisler's ideal observer because one of our primary interests was in determining the extent to which scotopic contrast sensitivity is limited by pre-neural as opposed to neural factors. This ideal observer was originally specified for the fovea under photopic viewing conditions, so it was modified in order to derive an equivalent scotopic ideal observer. The mean packing density (Curcio, Sloan, Kalina & Hendrickson, 1990) and effective aperture of rods (Curcio, personal communication) were averaged over a stimulus area centered at 20 deg in the nasal visual field (NVF). The optical line spread function was estimated from the data of Jennings and Charman (1981) for best axial refraction and pupils dilated to about 7.5 mm. The quantum efficiency of rhodopsin, specified at the retina, was reported by Knowles (1982). The transmittance of the ocular media

TABLE 1. Parameters for the scotopic ideal discriminator

Factor	Source	Value
Mean rod density (20 deg temp. ret.)	C. Curcio	128,042 rods/mm^2
Rod effective aperture	C. Curcio	2.0 μm
Optical line spread (half-width)	Jennings and Charman	5.5 arc min
Rod quantum efficiency	A. Knowles	0.66
Media transmittance cornea, vitreous, and lens	Wyszecki and Stiles	Values depend on wavelength (e.g. $T = 0.4346$ at 505 nm)

as a function of wavelength and the absorptance spectrum of rhodopsin was derived from standard tables (Wyszecki & Stiles, 1982). The fraction of quanta entering rods that is absorbed by rhodopsin was obtained from Alpern and Pugh (1974) and Zwas and Alpern (1976). The values used for these parameters are shown in Table 1 (see also Appendix A).

Experiment 1

Methods

As in other studies of photopic contrast sensitivity (Banks *et al.*, 1987; Banks, Sekuler & Anderson, 1991), it was important to minimize the effects of grating summation area. The ideal observer, unlike human observers, can summate information over the largest possible grating patch. Thus, to facilitate comparisons of human and ideal performance, target sizes were selected that were no larger than the grating summation area of humans. A photopic study by Howell and Hess (1978) found that, while summation took place over a constant number of cycles (7–10) for higher spatial frequencies, the sensitivity plateau was reached at fewer cycles for spatial frequencies below 1 cpd. Hoekstra, van der Goot, van den Brink and Bilsen (1974) found that the sensitivity plateau was reached at fewer cycles as the mean light level decreased. Taken together, the two latter studies suggest that sensitivity might asymptote at a smaller number of cycles under scotopic conditions when spatial frequency and light level are both low. Consequently, an experiment was conducted to determine the relationship between sensitivity and patch size under the conditions of interest.

Square grating patches were used. As the number of cycles was increased, the bar length was increased by the same amount. The spatial frequencies of the grating patches were 0.125, 0.25, 0.5, 1 and 2 cpd, numbers of cycles were 1, 2, 4, 6, 8 and 12, and space-average illuminances were -1.16 and -0.21 log scot td for observer GS and -1.27 log scot td for observer SS. The measurements at 2 cpd were possible only at the higher light level and gratings of 8 and 12 cycles were presented at spatial frequencies of 0.5, 1 and 2 cpd only.

Results

Figures 1 and 2 show for both observers how contrast sensitivity varied with the extent of the sinewave gratings (quantified in cycles for grating height and width). Each curve in a given panel represents the results for a different spatial frequency. Three aspects of these grating summation data are noteworthy. First, the lower the spatial frequency, the fewer the number of cycles needed

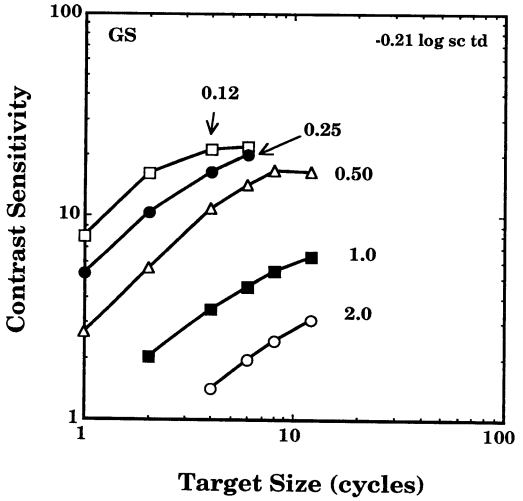

FIGURE 1. Grating summation results for subject GS at -0.21 log scot td for five indicated spatial frequencies. Height and width of target expressed in cycles.

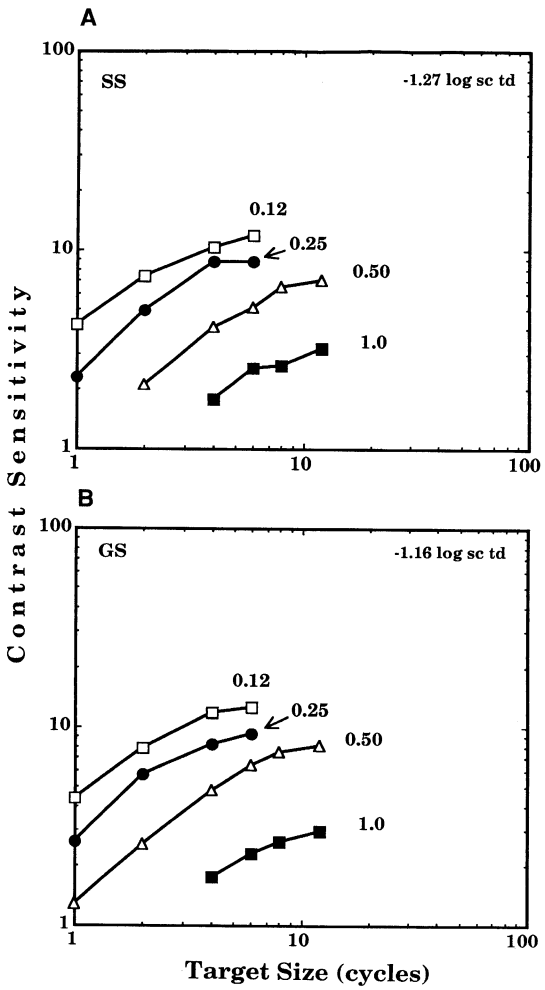

FIGURE 2. Grating summation results at four spatial frequencies for two observers. Height and width of target expressed in cycles. (A) Data for subject SS at -1.27 log scot td. (B) Data for subject GS at -1.16 log scot td.

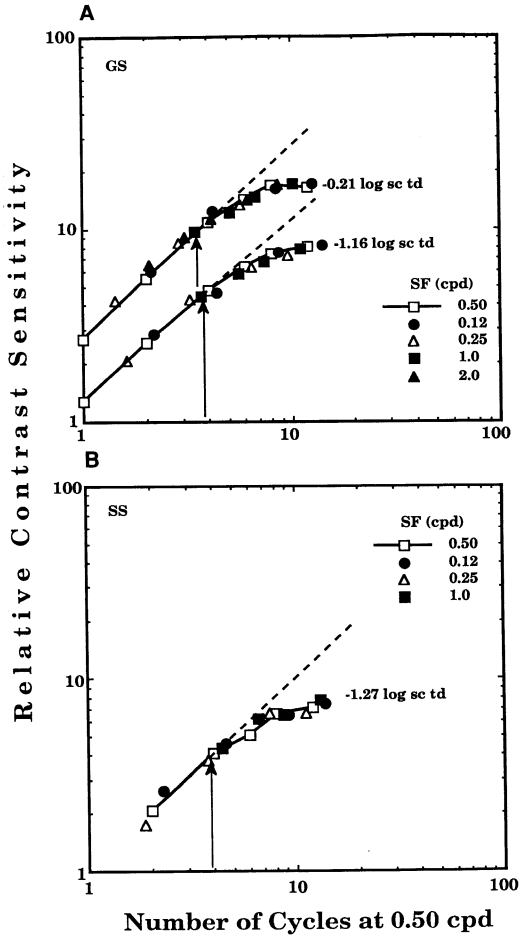

FIGURE 3. Grating summation data fit to 0.50 cpd curve by translation along the vertical and horizontal axes. No rotation was permitted. Point at which the slope of the best-fitting curve first fell below 1 (indicated by the arrow) represents the "equivalent" number of cycles at various frequencies. (A) Data for subject GS at −0.21 and −1.16 log scot td. (B) Data for subject SS at −1.27 log scot td.

to reach the plateaux. For instance, 8–12 cycles were needed at 1 cpd to approach the plateau, whereas only 4–6 cycles were required at 0.25 cpd. Second, summation does not vary much with illuminance over the 1 log-unit range used here. Third, the shapes of the summation curves are similar for all spatial frequencies, light levels, and both observers.

These results were used to determine the "equivalent" number of cycles for each condition of the main experiment. In order to determine the equivalent number, the data were shifted vertically and horizontally to achieve the best match to a curve fit to the 0.50 cpd data. Figure 3(A) shows the shifted data of observer GS at two light levels and Fig. 3(B) shows similar data for observer SS at the one light level. The data for each respective light level clearly superimpose, which shows that the shapes of the summation curves within both of the first two figures are similar. The points (indicated by the arrows) at which the slope of the best-fitting curve first fell below one (represented by the dashed line) were used to determine the "equivalent" number of cycles at various frequencies. "Equivalence" simply means that the resulting sensitivities are at comparable positions on the respective grating summation slopes.

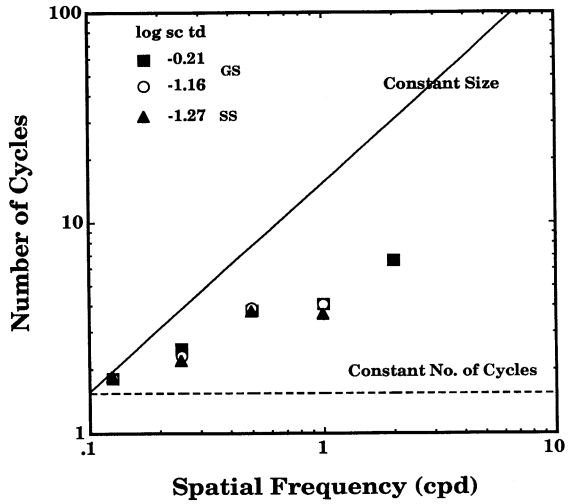

FIGURE 4. Equivalent number of cycles for different spatial frequencies obtained from grating summation area measurements at −0.21 and −1.16 log scot td for subject GS and −1.27 log scot td for subject SS.

Figure 4 plots the equivalent number of cycles (the number of cycles indicated by the arrows in Fig. 3) vs spatial frequency for both light levels for subject GS and one light level for subject SS. The data points are nearly identical for the different light levels and both subjects. Straight lines were fit by eye to the data in Fig. 4 in order to determine the equivalent number of cycles for each light level. These estimates (taken as ±1 SD of the Gabor patch) were doubled to determine the full height and width of Gabor patches (±2 SD) in the "equivalent cycles" CSF experiment described below (see Appendix B).

Experiment 2

Methods

Contrast sensitivity was measured with Gabor patches whose size was selected according to either the equivalent or constant number of cycles strategy. Four cycles were always presented in the constant number of cycles measurements. Various numbers of cycles ranging from 3.6 to 9 cycles, determined from the grating summation data, were presented in the equivalent number of cycles measurements. Testing was conducted at three low light levels, all of which were shown to be truly scotopic. A fourth light level, thought to be mesopic, was used in the CSFs measured with a constant number of cycles for purposes of comparison. Because the dilated pupil size differed for the two observers, their retinal illuminances were accordingly different. The retinal illuminances, expressed in log scot td and, in parentheses, log phot td were:

observer GS:
0.88 (−0.70), −0.21 (−1.70), −1.40 (−2.70), −2.49 (−3.70)

observer SS:
0.77 (−0.81), −0.32 (−1.81), −1.51 (−2.81), −2.60 (−3.81)

Because we wished to obtain some measurements at as high a spatial frequency as possible, both our stimuli and psychophysical method were altered to permit testing at a contrast greater than 100%. Gaussian-damped rectangular waves were generated with a duty cycle of 0.25 to permit testing at spatial frequencies at or beyond the cut-off frequency as conventionally measured (generally about 1 cpd or higher). By this maneuver, a contrast of 150% was produced for the fundamental frequency, the higher harmonics being invisible. Instead of varying contrast as in the two-interval, forced-choice paradigm, the contrast was fixed at 150% and the spatial frequency was varied by changing the test distance. A yes–no paradigm with 50% catch trials was utilized to generate psychometric functions. The spatial frequency corresponding to 75% correct, obtained from probit analysis, was taken as threshold.

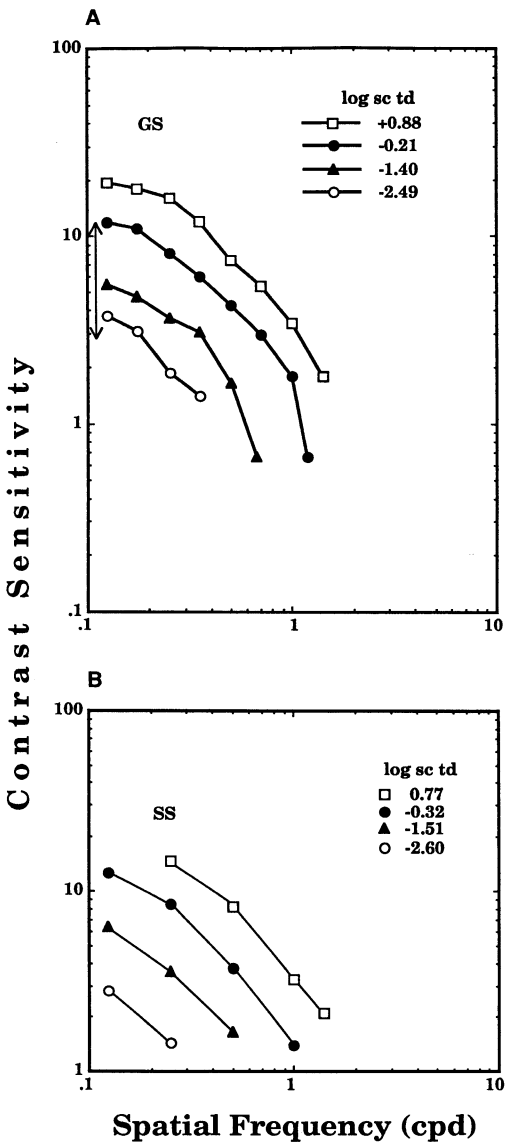

FIGURE 5. Contrast sensitivity measured with 4-cycle Gabor patches at four light levels. (A) Data for subject GS; arrow indicates the predicted change in sensitivity in going from −0.21 to −1.40 log scot td if subject had obeyed square-root law for luminance. (B) Comparable data for subject SS.

Results

CSFs with a constant number of cycles. CSFs were measured using 4-cycle Gabor patches. Figure 5 shows the results for both observers at four light levels. There was probably some cone intrusion at the highest light level, but the data was plotted for comparison nonetheless. The constant-cycle CSF is clearly low-pass in all cases. As light level is decreased, sensitivity decreases at all spatial frequencies. The arrow in Fig. 5(A) shows the sensitivity change one would expect when illuminance is changed from −0.21 to −1.40 log scot td if the subject obeyed square-root (DeVries–Rose) law. Clearly, sensitivity changed much less than expected from square-root law.

Figure 6 plots contrast sensitivity as a function of light level for a variety of spatial frequencies. The horizontal line in Fig. 6(A) represents Weber behavior, meaning no change in contrast sensitivity with light level. The straight line with slope of 0.5 represents square-root, or DeVries–Rose, behavior, which is the behavior of ideal observers limited by photon noise. These lines have been arbitrarily positioned vertically to allow comparison with the slopes of human behavior. Data for subject GS is shown for four spatial frequencies; nearly identical

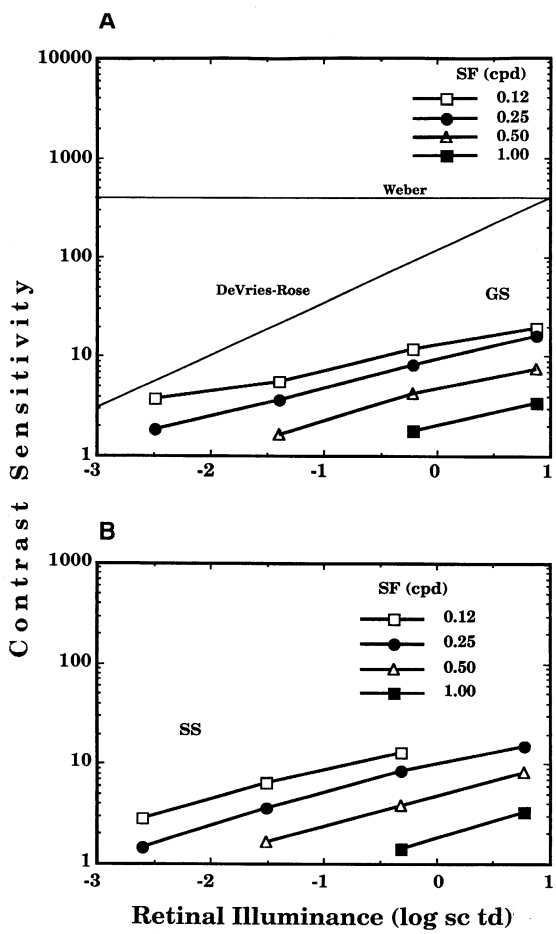

FIGURE 6. Contrast sensitivity as a function of retinal illuminance for four spatial frequencies. (A) Data for subject GS; horizontal line represents Weber behavior and diagonal line with slope of 0.5 indicates DeVries–Rose behavior. (B) Data for subject SS.

slopes were found for subject SS. The slope of our observers' data was about 0.25, which falls between Weber and DeVries–Rose behavior.

CSFs with equivalent number of cycles. CSFs for both observers were also measured using the "equivalent" number of cycles strategy. Figure 7 shows the results for observer GS at three light levels and for observer SS at two light levels. Because the "equivalent" cycles strategy generally required more than 4 cycles in the Gabor patch (at full height and width), contrast sensitivities were higher with this strategy than with the 4-cycle patches. Because the "equivalent" number of cycles may yield more realistic comparisons of relative sensitivities across spatial frequencies *per se* (Howell & Hess, 1978; Banks *et al.*, 1987), these data are emphasized in our comparisons of human and ideal performance.

Comparison of human to ideal performance. Figures 8 and 9 display the results for both observers at two light levels and the performance of the ideal discriminator under the same conditions. As expected, ideal sensitivity was invariably greater than that of human observers. It is of theoretical interest to know if the shapes of the human and ideal CSFs are similar (Banks *et al.*, 1987, 1991). The ideal sensitivity curve (for the equivalent number of cycles condition at −0.21 log scot td) was shifted down the log sensitivity axis in Fig. 10 to facilitate comparison with the human data (observer GS) at that same light level. Human performance peels away from ideal at both ends of the range of spatial frequencies tested.

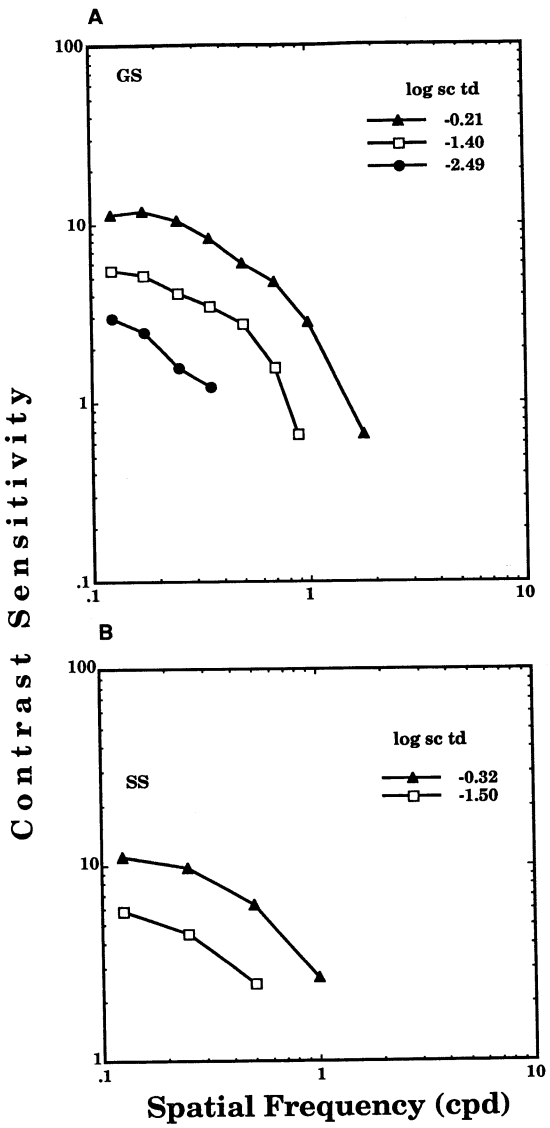

FIGURE 7. Contrast sensitivity measured with Gabor patches having the equivalent number of cycles (determined from the grating summation experiment) within ±1 SD. Full height and width of patches was ±2 SD; see Appendix B for patch sizes for each spatial frequency. (A) Data shown for subject GS at three scotopic light levels. (B) Data for subject SS at two light levels.

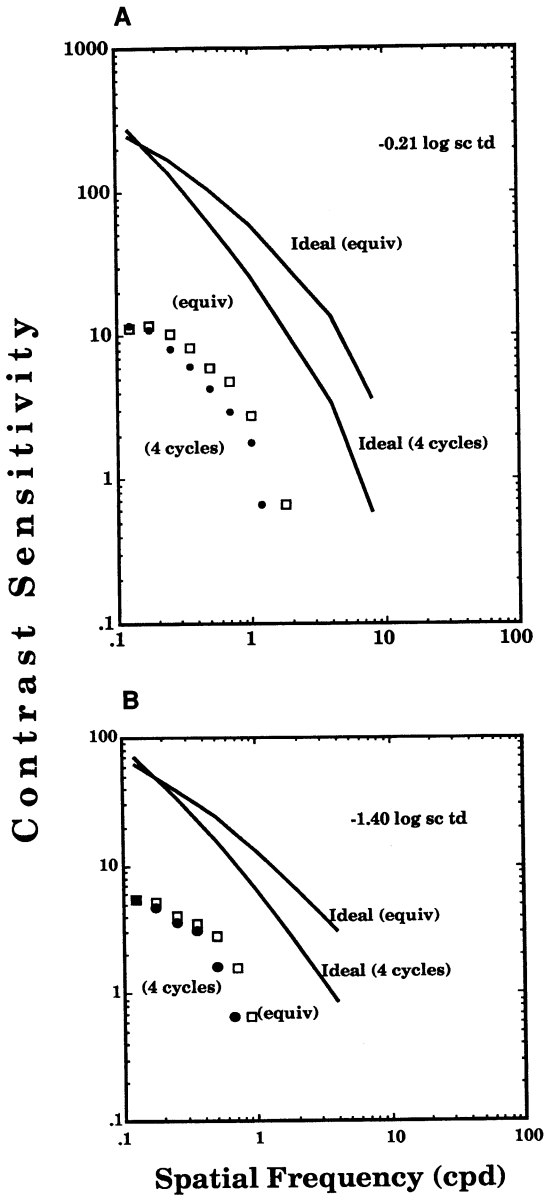

FIGURE 8. Contrast sensitivities for four cycle patches vs "equivalent" number of cycles. Symbols represent data for subject GS; solid lines represent performance of the ideal discriminator. (A) Results at −0.21 log scot td; for spatial frequencies beyond 1.0 cpd, Gaussian-damped rectangular waves which produced 150% contrast were utilized. (B) Results at −1.40 log scot td.

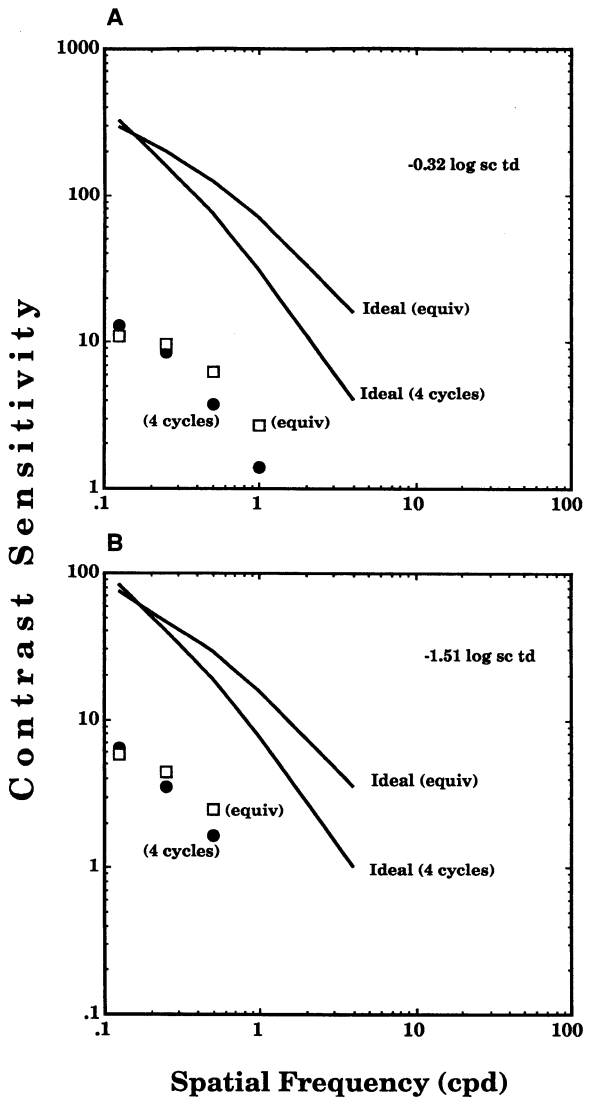

FIGURE 9. Contrast sensitivities for four cycle patches vs "equivalent" number of cycles. Symbols represent data for subject SS; solid lines represent performance of the ideal discriminator. (A) Results at −0.32 log scot td. (B) Results at −1.51 log scot td.

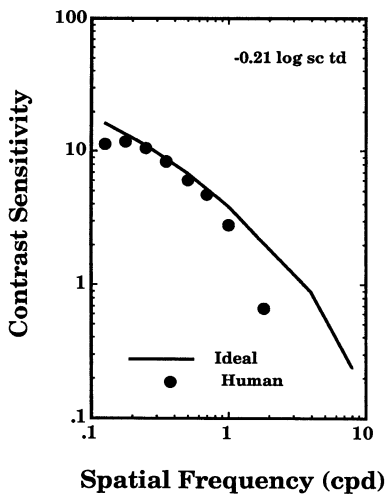

FIGURE 10. The ideal discriminator's performance, represented by the solid curve, has been slid vertically down the log sensitivity axis to facilitate a comparison with human CSF; solid symbols represent data from subject GS at −0.21 log scot td.

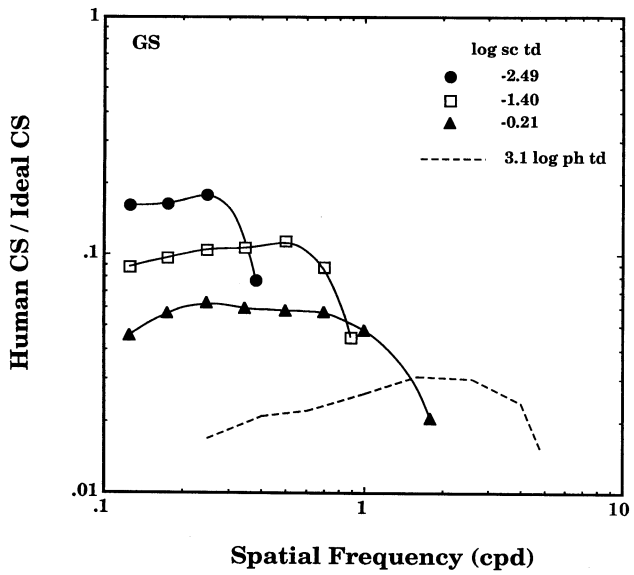

FIGURE 11. The ratio of human/ideal contrast sensitivities ("neural efficiency functions") for subject GS at three light levels. Data is shown for the equivalent number of cycles strategy. The dashed curve shows data for photopic lighting but otherwise similar conditions (Banks *et al.*, 1991).

DISCUSSION

The contrast sensitivity of human observers under scotopic viewing conditions was investigated and compared to the best possible (ideal) sensitivity if all the information at the output of the rods was used optimally. Naturally, human contrast sensitivity was found to be lower than that of such an ideal observer. Our main interest was in investigating the following three aspects of scotopic efficiency, as indexed by the ratio of human/ideal contrast sensitivity (with ideal observer at the receptors):

(1) How does scotopic efficiency vary with light level?
(2) How does it vary with spatial frequency?
(3) How does it compare to photopic efficiency?

Scotopic efficiency and retinal illuminance

Figure 11 displays the human/ideal contrast sensitivity ratios at the three light levels tested. The dashed curve shows data for similar conditions but for photopic lighting (Banks *et al.*, 1991). The ratios clearly vary with light level, i.e. the curves do not superimpose. The highest ratios were observed at −2.5 log scot td, the lowest level tested. Ideal sensitivity always increased as the square root of the space-averaged luminance, following square-root, or DeVries–Rose, law. The fact that human/ideal ratios vary with retinal illuminance shows that human contrast sensitivity does not follow square-root law under our scotopic conditions. This point was emphasized in Fig. 6 where approximately "fourth-root" behavior was demonstrated.

Hess (1990) pointed out that a number of studies of contrast sensitivity under scotopic conditions have reported DeVries–Rose behavior at lower scotopic levels with a transition to Weber behavior at higher scotopic levels. However, Koenderink, Bouman, Bueno

de Mesquita and Slappendel (1978) found a slope intermediate to these two behaviors for certain combinations of spatial and temporal frequency over a range of scotopic light levels, as did Kelly (1972) for low photopic conditions. The effect of luminance on contrast sensitivity may depend on the spatial and temporal properties of the stimulus, as well as retinal eccentricity. In any event, there is no question that under our testing conditions, the contrast sensitivity of human observers followed a rule intermediate to DeVries–Rose and Weber behavior (i.e. fourth-root performance).

Scotopic efficiency and spatial frequency

We wanted to determine if pre-neural factors could account for the shape of the scotopic CSF like they did for photopic foveal CSFs (Banks *et al.*, 1987). The human/ideal sensitivity ratios (see Fig. 11) were not constant as a function of spatial frequency which means that pre-neural factors along with grating summation area cannot account for the shape of the scotopic CSF. Some post-receptoral site, perhaps the retinal ganglion cells (Banks *et al.*, 1991) must therefore act as a low pass filter. Notice further that the spatial frequency at which the ratio of human/ideal contrast sensitivity falls off is much lower at −2.49 log scot td than at −0.21 log scot td. This suggests that, if a single post-receptoral filter is responsible for the high-frequency roll-off in these sensitivity ratios, it would have to change its spatial properties significantly as a function of light level. This observation is at least qualitatively consistent with reports of how center and surround mechanism sensitivities of retinal ganglion cells and lateral geniculate cells are affected differently by light adaptation (Barlow & Levick, 1976; Kaplan, Marcus & So, 1979; Derrington & Lennie, 1982).

Scotopic vs photopic efficiency

The highest human/ideal sensitivity ratio obtained for this detection task, found at our lowest light level, was about 1:5 (0.18) for a spatial frequency of 0.25 cpd. Recent evidence presented by Banks *et al.* (1991) indicated that the photopic periphery (20 deg NVF) yielded human/ideal sensitivity ratios for detection of about 0.02 at 0.25 cpd, nine times worse than scotopic performance under otherwise comparable conditions. Even though scotopic contrast sensitivity is much lower than photopic, human/ideal sensitivity ratios for detection are significantly higher under scotopic conditions compared to photopic conditions.

Comparisons to other estimates of efficiency

While we have chosen human/ideal contrast sensitivity ratios as our metric of performance, another useful benchmark is quantum efficiency. There are a number of different ways of specifying this alternative metric. Watson *et al.* (1983) defined quantum efficiency as the ratio of ideal and empirical contrast energies. Because contrast energy is proportional to the square of the stimulus contrast (C), quantum efficiency (F) for our grating detection task can be calculated as follows:

$$F = (C_{\text{ideal}})^2/(C_{\text{human}})^2 \quad (1)$$

$$F = (CS_{\text{human}})^2/(CS_{\text{ideal}})^2. \quad (2)$$

Equivalently, for detection of a spot of light at absolute threshold Barlow (1962a, 1977):

$$F = \text{No. quanta}_{\text{ideal}}/\text{No. quanta}_{\text{human}}. \quad (3)$$

Using our highest human/ideal sensitivity ratio for detection of about 1:5 (0.18) in equation (2), we obtained a quantum efficiency of just over 3%. We wished to compare our quantum efficiency with that obtained at absolute threshold. Hecht, Shlaer and Pirenne's (1942) findings suggested that 5–14 isomerizations were needed to produce a visual event. This range of human thresholds and an ideal threshold of 0.9 were used in equation (3) to calculate quantum efficiency. This yielded a post-receptoral quantum efficiency of 6–18%, well above our 3% finding (see Appendix A for a discussion of the assumptions that underlie these calculations).

This prompted us to consider what conditions might bring human scotopic contrast sensitivity closer to ideal. We have already shown that efficiency is higher at lower light levels and lower spatial frequencies (see Fig. 11). Banks *et al.* (1987) noted that human performance more closely approached ideal in contrast discrimination than in contrast detection tasks. In a pilot experiment, a similar discrimination paradigm was used. The contrast of one Gabor patch, the pedestal stimulus, was fixed and the contrast of the other patch was varied until the observer could just discriminate which of the two patches had the greater contrast.

Figure 12 shows the results for a 4-cycle patch of 0.25 cpd. A dipper-like function is obtained for human observers analogous to results obtained under photopic conditions (Nachmias & Sansbury, 1974; Legge & Foley, 1980) and also under mesopic conditions (Bradley & Ohzawa, 1986). At the bottom of the dipper, where the pedestal contrast is near detection threshold, the increment threshold is 2.4%, about one-fifth the detection threshold. The horizontal line at 0.8% shows the behavior of the ideal observer. Notice that the ideal observer does not exhibit a pedestal effect. The ideal discriminator is strictly concerned with the difference in the weighted quantal catch between the two alternatives, so it does not matter whether the two alternatives are a Gabor patch and a uniform background, or two Gabor patches of differing contrast. The ratio of human/idea sensitivity is about 1:3 (0.33) at −0.21 log scot td. This ratio is slightly higher than the highest (0.25) reported by Crowell and Banks (1992) for contrast discrimination with one-cycle Gabor patches in the photopic fovea. The ratio of 1:3 corresponds to a quantum efficiency of about 11%, within the range of post-receptoral efficiencies we estimated for Hecht *et al.* (1942).

Banks *et al.* (1991) reported photopic human/ideal contrast sensitivity ratios ("neural efficiency functions")

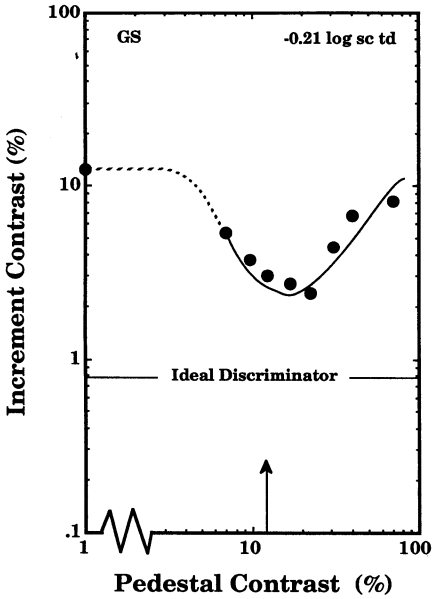

FIGURE 12. Contrast discrimination for subject GS at −0.21 log scot td. Stimuli were four cycle Gabor patches of 0.25 cpd. The arrow indicates the pedestal contrast which corresponds to detection threshold. The horizontal line shows the performance of the ideal discriminator on this same task.

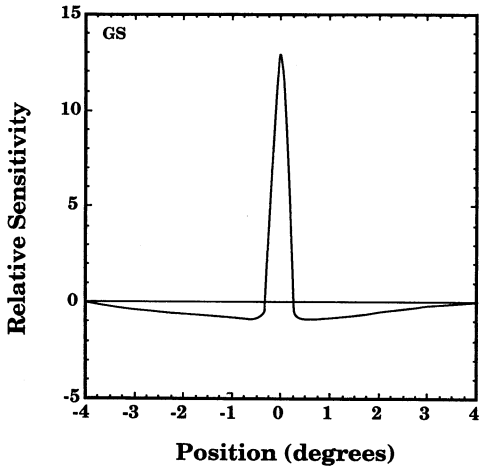

FIGURE 13. The neural sensitivity profile obtained by taking the inverse Fourier transform of the human/ideal contrast sensitivity ratios shown in Fig. 11 for subject GS at −0.21 log scot td.

for eccentric viewing that look much like those of Fig. 11 (see dashed curve). They hypothesized that the efficiency loss at high spatial frequencies was caused by pooling of cones onto higher-order neurons, perhaps retinal ganglion cells. They also estimated the amount of pooling that would be required to explain the high-frequency losses at each eccentricity. Here the same issue is considered under scotopic lighting. Smooth curves were fit to the neural efficiency functions of Fig. 11 and the inverse Fourier transforms were computed. If one assumes that this filter is the only type of limiting post-receptoral filter and that the system is linear, then the resultant is the impulse response of the limiting filter. Both of these assumptions are undoubtedly false in detail, but under our conditions they are accurate enough to justify this analysis. The profile of the inverse Fourier transform is shown in Fig. 13. This "neural sensitivity profile" has a width at half-height of 17 arc min and a large, shallow inhibitory surround.

Using the rod density data of Curcio *et al.* (1990), the number of rods required to fill the center mechanism of this presumed post-receptor filter was estimated. At half-height, the center mechanism would contain about 650 rods. To make this computation, it was assumed that the distribution and connectivity of rods was homogeneous across the retinal area tested. It was also assumed that the center mechanism was circularly symmetric.

The grating summation study also revealed an important aspect of scotopic vision. Similar to the photopic data of Howell and Hess (1978) for spatial frequencies of 1 cpd or less, our grating summation results clearly showed that the lower the spatial frequency, the fewer the number of cycles in the summation area. This suggests that psychophysical receptive (or, perceptive) fields are smaller in terms of the number of cycles for lower spatial frequencies. A similar relationship was found by Banks *et al.* (1991) in the periphery and by Anderson and Burr (1987) in the fovea.

CONCLUSIONS

Under scotopic conditions, grating summation area (in cycles) decreased with decreasing spatial frequency for frequencies below 2 cpd. Grating summation curves, translated vertically and horizontally, superimposed for all spatial frequencies tested.

Making use of a scotopic ideal observer, it was demonstrated that human performance on our contrast detection task converged on ideal behavior as light level was decreased. Pre-neural factors along with grating summation area could not account for the shape of the scotopic CSF. Under optimal conditions, scotopic efficiency (as indexed by the human/ideal contrast sensitivity ratio) was nine times higher than efficiencies at 20 deg eccentricity for contrast detection under photopic conditions. The highest human/ideal sensitivity ratio we obtained was 1:5 (0.18) for contrast detection and 1:3 (0.33) for contrast discrimination. Using physiologically plausible assumptions, it is estimated that the center mechanism of a single presumed post-receptoral filter would contain roughly 650 rods.

In terms of quantum efficiency, our contrast discrimination results yielded an efficiency of about 11% compared to an ideal discriminator placed at the photoreceptors. However, we believe that higher efficiencies might be attainable under optimal conditions: contrast discrimination of brief, small, low spatial frequency grating patches at low scotopic light levels. Under these conditions, the spatial, temporal and illuminance properties of the stimulus are most conducive to efficient processing by the retinal circuits and central visual pathways subserving scotopic vision.

REFERENCES

Alpern, M. & Pugh, E. N. Jr (1974). The density and photosensitivity of human rhodopsin in the living retina. *Journal of Physiology, London, 237*, 341–370.

Anderson, S. J. & Burr, D. C. (1987). Receptive field size of human motion detection units. *Vision Research, 27*, 621–635.

Banks, M. S., Geisler, W. S. & Bennett, P. J. (1987). The physical limits of grating visibility. *Vision Research, 27*, 1915–1924.

Banks, M. S., Sekuler, A. B. & Anderson, S. J. (1991). Peripheral spatial vision: Limits imposed by optics, photoreceptors, and receptor pooling. *Journal of the Optical Society of America, A, 8*, 1775–1787.

Barlow, H. B. (1956). Retinal noise and absolute threshold. *Journal of the Optical Society of America, 46*, 634–639.

Barlow, H. B. (1957). Increment thresholds at low intensities considered as signal/noise discriminations. *Journal of Physiology, London, 136*, 469–488.

Barlow, H. B. (1958). Temporal and spatial summation in human vision at different background intensities. *Journal of Physiology, London, 141*, 337–350.

Barlow, H. B. (1962a). A method for determining the overall quantum efficiency of visual discriminations. *Journal of Physiology, London, 160*, 155–168.

Barlow, H. B. (1962b). Measurements of the quantum efficiency of discrimination in human scotopic vision. *Journal of Physiology, London, 160*, 169–188.

Barlow, H. B. (1977). Retinal and central factors in human vision limited by noise. In Barlow, H. B. & Fatt, P. (Eds), *Vertebrate photoreception* (pp. 337–358). New York: Academic Press.

Barlow, H. B. & Levick, W. R. (1976). Threshold setting by the surround of cat retinal ganglion cells. *Journal of Physiology, London, 259*, 737–757.

Baumgardt, E. (1960). Mesure pyrometrique du seuil visuel absolu. *Optica Acta, 7*, 305–316.

Bouman, M. A. (1955). Absolute threshold conditions for visual perception. *Journal of the Optical Society of America, 45*, 36–43.

Bradley, A. & Ohzawa, I. (1986). A comparison of contrast detection and discrimination. *Vision Research, 26*, 991–997.

Crowell, J. A. & Banks, M. S. (1992). The efficiency of foveal vision. *Journal of the Optical Society of America, A*. Submitted.

Curcio, C. A., Sloan, K. R., Kalina, R. E. & Hendrickson, A. E. (1990). Human photoreceptor topography. *Journal of Comparative Neurology, 292*, 497–523.

Daitch, J. M. & Green, D. G. (1969). Contrast sensitivity of the human peripheral retina. *Vision Research, 9*, 947–952.

Denton, E. J. & Pirenne, M. H. (1954). The absolute sensitivity and functional stability of the human eye. *Journal of Physiology, London, 123*, 417–442.

Derrington, A. M. & Lennie, P. (1982). The influence of temporal frequency and adaptation level on receptive field organization of retinal ganglion cells in cat. *Journal of Physiology, London, 333*, 343–366.

Geisler, W. S. (1984). Physical limits of acuity and hyperacuity. *Journal of the Optical Society of America, A1*, 775–782.

Geisler, W. S. (1989). Sequential ideal-observer analysis of visual discriminations. *Psychological Review, 96*, 267–314.

Geisler, W. S. & Davila, K. D. (1985). Ideal discriminators in spatial vision: Two point stimuli. *Journal of the Optical Society of America, A2*, 1483–1497.

Hallett, P. E. (1969). Quantum efficiency and false positive rate. *Journal of Physiology, London, 202*, 421–436.

Hallett, P. E. (1987). Quantum efficiency of dark-adapted human vision. *Journal of the Optical Society of America, A4*, 2330–2335.

Hecht, S., Shlaer, S. & Pirenne, M. H. (1942). Energy, quanta, and vision. *Journal of General Physiology, 25*, 819–840.

Hess, R. F. (1990). The Edridge-Green Lecture. Vision at low light levels: Role of spatial, temporal and contrast filters. *Ophthalmic and Physiological Optics, 10*, 351–359.

Hoekstra, J., van der Goot, D. P. J., van den Brink, G. & Bilsen, F. A. (1974). The influence of the number of cycles upon the visual contrast threshold for spatial sine wave patterns. *Vision Research, 14*, 365–368.

Howell, E. R. & Hess, R. F. (1978). The functional area for summation to threshold for sinusoidal gratings. *Vision Research, 18*, 369–374.

Jennings, J. A. M. & Charman, W. N. (1981). Off-axis image quality in the human eye. *Vision Research, 21*, 445–455.

Jones, R. C. (1959). Quantum efficiency of human vision. *Journal of the Optical Society of America, 49*, 645–653.

Kaplan, E., Marcus, S. & So, Y. T. (1979). Effects of dark adaptation on spatial and temporal properties of receptive fields in cat lateral geniculate nucleus. *Journal of Physiology, London, 294*, 561–580.

Kelly, D. H. (1972). Adaptation effects on spatio-temporal sine-wave thresholds. *Vision Research, 12*, 89–101.

Knowles, A. (1982). The biochemical aspects of vision. In Barlow, H. B. & Mollon, J. D. (Eds), *The senses* (pp. 82–101). Cambridge: Cambridge University Press.

Koenderink, J. J., Bouman, M. A., Bueno de Mesquita, A. E. & Slappendel, S. (1978). Perimetry of contrast detection thresholds of moving spatial sine wave patterns. IV. The influence of the mean retinal illuminance. *Journal of the Optical Society of America, 68*, 860–865.

Legge, G. E. & Foley, J. M. (1980). Contrast masking in human vision. *Journal of the Optical Society of America, 70*, 1458–1471.

van Meeteren, A. (1978). On the detective quantum efficiency of the human eye. *Vision Research, 18*, 257–267.

van Meeteren, A. & Boogaard, J. (1973). Visual contrast sensitivity with ideal image intensifiers. *Optik, 37*, 179–191.

Nachmias, J. & Sansbury, R. V. (1974). Grating contrast: Discrimination may be better than detection. *Vision Research, 14*, 1039–1042.

van Norren, D. & Vos, J. J. (1974). Spectral transmission of the human ocular media. *Vision Research, 14*, 1237–1244.

Pelli, D. G. (1990). The quantum efficiency of vision. In Blakemore, C. (Ed.), *Vision: Coding and efficiency*. Cambridge: Cambridge University Press.

Rose, A. (1948). The sensitivity performance of the human eye on an absolute scale. *Journal of the Optical Society of America, 38*, 196–208.

Sakitt, B. (1972). Counting every quantum. *Journal of Physiology, London, 223*, 131–150.

Savage, G. L. & Banks, M. S. (1988). Scotopic contrast sensitivity: Real vs ideal performance. *Investigative Ophthalmology and Visual Science (Suppl.), 26*, 59.

Wald, G. (1945). Human vision and the spectrum. *Science, 101*, 653–658.

Watson, A. B., Barlow, H. B. & Robson, J. G. (1983). What does the eye see best? *Nature, 302*, 419–422.

Wyszecki, G. & Stiles, W. S. (1982). *Color science: Concepts and methods, quantitative data and formulae* (2nd edn, pp. 592, 718–719, 789). New York: Wiley.

Zwas, F. & Alpern, M. (1976). The density of human rhodopsin in the rods. *Vision Research, 16*, 121–128.

Acknowledgements—We thank Christine Curcio for providing preprints of her data on the effective apertures of rods and cones as well as their distribution across the human retina, Bill Geisler for his assistance in installing his SDE software, Stan Klein for the use of his workstation, Tony Adams for help in the verification of rod isolation, and Sherry Savage for her dedicated service as an experimental subject in this study. This report was supported by NIH research grant HD-19927 to MSB.

Appendix A and B—overleaf

APPENDIX A

Our estimate of photometric efficiency was based on factors listed in Table 1.

A figure for media transmittance of 0.435 at 505 nm was obtained using the following data from Wyszecki and Stiles (1982) for large pupils: lens density = 0.115 + 0.15 (for conversion to absolute density) = 0.265. This absolute density yields a transmittance of 0.543 which, in turn, was multiplied by a 0.8 to allow for light loss due to reflection, absorption, and wide-angle scatter by the cornea and vitreous. No allowance was made for macular pigment since testing was conducted at 20 deg eccentricity.

Using an estimate of a mean rod effective aperture of 2.0 μm (Curcio, personal communication) and a mean rod density of 128,042 rods/mm^2 (Curcio *et al.*, 1990) at 20 deg temporal retina. Our calculations indicated that effective rod coverage was 0.417, less than the commonly cited value of 0.7 from Denton and Pirenne (1954). The balance of the retinal area was taken up by cones (0.230) and extra-cellular space (0.353).

The fraction of quanta entering rods that is absorbed by rhodopsin was taken to be 0.55, derived from Alpern and Pugh (1974) and Zwas and Alpern (1976).

The final factor is the fraction of absorbed quanta that result in an isomerization; a value of 0.66 was advocated by Knowles (1982).

Our overall "photometric efficiency" was computed by multiplication of these factors:

photometric efficiency (@ 507 nm) = 0.435*0.417*0.55*0.66 = 0.066 (or 6.6%).

Barlow (1977) estimated that photometric efficiency was higher, ranging from 11 to 33%. His high-end estimate of 33% was based in part on an effective rod coverage of 0.8 and a fraction of quanta absorbed that result in an isomerization of 1.0. While these values would be considered high relative to the more recent studies cited above, it is worthwhile to consider how a higher photometric value would influence our indices of efficiency. The ideal discriminator would increase in sensitivity by the square root of the ratio 33%/6.6%, or a factor of about 2.2 times more sensitive than our original estimate. This would reduce our best human/ideal sensitivity ratio (for contrast discrimination) from 0.33 to 0.15, and decrease quantum efficiency from 11% to about 2% based on the second equation in the text.

APPENDIX B

The following grating patch sizes, derived from the grating summation study, were used in the "equivalent number of cycles" CSF experiment:

Spatial frequency (cpd)	Full widths of Gabor patches (in cycles)	
	−0.21 log scot td	−1.16 log scot td
0.125	3.6	3.4
0.175	4.2	4.0
0.250	4.9	4.6
0.350	5.7	5.3
0.500	6.7	6.2
0.700	7.8	7.0
1.000	9.0	—